

Extraction of creatinine by adsorption onto pure micro- and mesoporous silica materials

Ghazala Benbakhta¹, Mustapha Mokhtari¹, Hadj Hamaizi^{1, *}, María Martínez Galera², María Dolores Gil García²

¹Department of Chemistry, College of Sciences, University of Oran1, Oran-Menaouer 31000, Algeria.

²University of Almería, La Cañada San Urbano S/N 04120 Almería, España.

Received: July 17, 2017; accepted: September 20, 2017.

This report describes the compositional and structural design strategy of a micro- and mesoporous silica materials mesh for the efficient removal of uremic toxins towards blood purification application. A series of mesoporous textured amorphous silica powdered samples have been prepared using non-ionic polyoxyethylene alkali surfactants which are inexpensive, biodegradable, and non-toxic materials. A cubic structure and a more or less orderly porosity are obtained from a highly acidic reaction mixture using tetraethylorthosilicate (TEOS) As expected, the nature of the surfactant used (i.e. $C_nH_{2n+1}(EO)_x-OH$ type) influences the porous structure and leads to pores in the order of 2 (microporous) to 4 nm (mesoporous) in addition to thick silica walls. Calcined materials lead amorphous silica with no toxicity; therefore, they have the potential to be utilized as a new approach to removing creatinine selectively from the bloodstream.

Keywords: synthesis; mesoporous silica; creatinine; adsorption.

***Corresponding author:** Hadj Hamaizi, Department of Chemistry, College of Sciences, University of Oran1, P.O. Box 1524, Oran-Menaouer 31000, Algeria. Phone: +213 550 462417. E-mail: hamaizimizou@yahoo.fr.

Introduction

Creatinine is a chemical waste molecule that it is generated from muscle metabolism when creatine breaks down. Creatinine is one of the substances that kidneys normally eliminate from the body. High levels of creatinine may indicate that the kidney is damaged and not working properly. A creatinine blood test measures the level of creatinine in the blood. Kidney failure causes dangerous concentrations of waste products, such as potassium, urea and creatinine, to build-up in the body. Apart from having a kidney transplant, the next best solution for patients is dialysis, which is tedious. It is time-consuming and relies on access to specialist equipment, and, usually, a hospital. Often these requirements aren't accessible in

rural parts of developing countries and disaster areas.

Easily treatments based on adsorption were proposed by Bergé-Lefranc et al. [1, 2] and showed that creatinine adsorption which is the highest when adsorbed from pure water, is reduced when adsorbed from sodium chloride solution or from physiological buffered saline solutions. Once adsorbed, creatinine is present in protonated form within the zeolite, in equilibrium with other cations of the medium. Adsorption properties of zeolites and active carbons [3-7] show that adsorption capacities of uremic toxins over Faujasite (HFAU) and Beta (HBEA) have been evaluated by varying the composition of solvent by using water, physiological, and sodium chloride solutions.

HFAU was found to be more efficient in adsorption of these molecules. The adsorption results over HFAU were compared in various conditions to understand the adsorption mechanism. Thus, the adsorption mechanism was confirmed also by Fourier transform infrared and X-ray diffraction analysis, and it is found to be through the interaction of creatinine by hydrogen bonding on two types of sites on zeolites.

Diffuse reflectance UV spectroscopy was used to quantify the amount of creatinine adsorbed onto mordenite type zeolite. Quantification by diffuse reflectance UV spectroscopy after microporous solids extraction was linearly correlated with creatinine concentration whatever the medium. Finally, hydrophobic HFAU zeolite seems to be an efficient adsorbent; it is able to be easily regenerated under air, through retention of these initial adsorption properties. It is possible to eliminate 75% creatinine by adsorption onto an acidic mordenite (MOR) and 60% p-cresol by adsorption onto a hydrophobic silicalite (MFI). These results are comparable or better than conventional dialysis systems where the elimination is about 67% for creatinine and about 29% for p-cresol. Adsorption of uremic toxins onto active carbon is equal or better than onto zeolites, however, the application of this adsorbent has to be rejected as adsorption is non-specific.

Mechanism of creatinine adsorption was also studied recently by Nakemawa et al. [8] and Takai et al. [9] which develop and describe a nanofiber mesh that soaks up creatinine, this is an important step towards a portable blood purification system. They prepared a zeolite-polymer hybrid nanofiber mesh using a blood-compatible polymer, poly (ethylene-co-vinyl alcohol) (EVOH) demonstrated elsewhere as biomaterial [10-12]. Authors trapped a zeolite into a composite mesh by electrospinning it with the biocompatible polymer, poly-(ethylene-co-vinylalcohol), to prevent the zeolite from being released into the bloodstream. They then tested the ability of the composite mesh to adsorb

creatinine from solution. The team had worried that the properties of EVOH would disable the adsorption properties of the zeolite, but instead they found the adsorption capacity of the mesh was 67% of the free zeolites. The greatest challenge was precisely controlling the crystallinity of the polymer-zeolite fibers so that they were both insoluble and hydrophilic. The fibers have to be hydrophilic so that the uremic toxin could access the embedded zeolites, but hydrophilic fibers are not stable in water.

Mesoporous materials have opened many new possibilities for applications in catalysis, separation, and nanoscience due to their large, controllable pore sizes and high surface areas. The pore structure, such as channel connectivity and pore size of the mesoporous materials is one of the most important physical parameters of these materials for practical applications and must be designed depending on their uses [13-19].

In a brief history on these materials made from nonionic surfactants as structure-directing agents, we note two notable types of mesostructured oxides which have been prepared using assembly mechanisms involving hydrogen-bonding interactions of neutral precursors with nonelectrostatic surfactants [20-23]. The first of these mechanisms denoted S⁰I⁰, utilized primary alkylamines as structure-directing agents [20, 21]. Silica mesostructures formed by this process were denoted HMS silica. The second nonelectrostatic mesostructure assembly route, denoted N⁰I⁰, involved the use of nonionic surfactants, including alkylpoly (ethylene oxide) diblock copolymer surfactant, bis (poly(ethylene oxide))polypropylene triblock copolymer surfactants, and ethoxylated sorbitan esters [22-29]. Siliceous materials formed by this pathway were designated as MSU-X materials. Using both S⁰I⁰ and N⁰I⁰ mechanisms, mesoporous materials related to those formed by electrostatic assembly are obtained, but with more disordered framework structures resulting. Kim et al. [28] studied the formation of mesoporous silica materials using blends of

diblock copolymers $C_nH_{2n+1}(OCH_2CH_2)_x-OH$, verifying that mesostructure of the silica materials changes as the volume of the hydrophilic EO group of the surfactant increases, from lamellar to two-dimensional hexagonal ($p6mm$), three-dimensional hexagonal, a cubic phase, and another cubic phase with $Im\bar{3}m$ symmetry.

The research reported here extends this all previous work to improve the creatinine adsorption onto amorphous purely silica materials mesostructured. These solids have both a micro- and mesoporosity texture. Ordered silica mesoporous/microporous particles have been obtained by a facile protocol of preparation in acidic medium using polyoxyethylene ethers. Samples freshly obtained and calcined are used for the adsorption of creatinine by a formula using serum (blood) creatinine level. At ambient temperature and neutral pH, the adsorption capacities of these materials were up to 1 mg/g and being appreciate adsorbents.

Material and methods

1. Chemicals

Polyethylene glycol tert- octylphenyl ether with linear formula $(C_2H_4O)_nC_{14}H_{22}O$, $n = 7$ or 8 named Triton™ X-114, Polyoxyethylene (100) stearyl ether with formula $C_{18}H_{37}(OCH_2CH_2)_nOH$, $n \approx 100$ named Brij® S 100 and tetraethylorthosilicate ($Si(OC_2H_5)_4$) TEOS were purchased from Aldrich-Sigma, USA. Detailed nomenclature including chemical formulas of the whole surfactants used is given in Table 1. Deionized water and hydrochloric acid (HCl 1 mol/l) have been used for each synthesis; the HCl 1 mol/l was prepared from 37% fuming hydrochloric acid (Aldrich-Sigma).

2. Synthesis of sorbents

Easy protocol of synthesis consists in a mixing of an aqueous solution of the surfactant with HCl 1 mol/l solution under constant stirring for 1 hour. The requisite amount of TEOS was added by

stirring for 24 hours at room temperature. The mixture was then heated at 353K (or 373K) overnight without stirring. The precipitated solid product was recovered by filtration, washed and dried at 353K. For example, 2 g of Triton™ X-114 in 30 g of deionized water were stirred for 10 minutes before adding 120 ml of HCl 1 mol/l solution. An amount of TEOS (9 g) was added to this homogeneous mixture and kept under vigorous stirring for 24 hours. The mixture was then introduced into a sealed tube and heated at 373K for 48 hours. The resulting white precipitates were filtered out, washed with copious amounts of H_2O , and allowed to air dry at room temperature for 24 h. The surfactant was removed by calcinations in air at 823K for 4h. This temperature was reached with a heating rate of $10^\circ C/min$ and a first plateau at 373K for 1h. After the second plateau at 823K for 4 hrs, the oven was cooled down at room temperature with a cooling rate of about $5K/min$ and a fine white powder was recovered. Samples are named X2-48-80 and X5-48-80 from synthesis using 2 g and 5 g of Triton X114 respectively, heated at 353K for 48h. Samples obtained from Brij® S100 are named BG-3-1 and BG-6-1 by using 3 g and 6 g of surfactant.

3. Characterization methods

Small-angle X-ray diffraction (XRD) patterns were recorded on an EMPYREAN PANalytical X-ray powder diffraction (XRD) using $Cu K\alpha$ radiation ($\lambda = 0.15418$ nm) in the 2θ range of $0.5-20^\circ$ with a scanning rate of $0.5^\circ/min$. The X'PERTPLUS© software enabled the counting of the spectra and the calculation of pore-pore distance by indexing the reflections. The N_2 isotherms were measured by automated apparatus ASAP 2020 (Micromeritics) at 77K. Prior to N_2 adsorption analysis; the samples were degassed at 673K for 4h. The BET surface areas were calculated based on the linear part of the BET plot (P/P_0 : 0.05–0.35). The total pore volumes were estimated according to nitrogen uptake at a relative pressure (P/P_0) of ca. 0.990. The pore size distribution and pore diameter were derived from the desorption branch of the N_2 isotherms using Barrett-Joyner-Halenda (BJH)

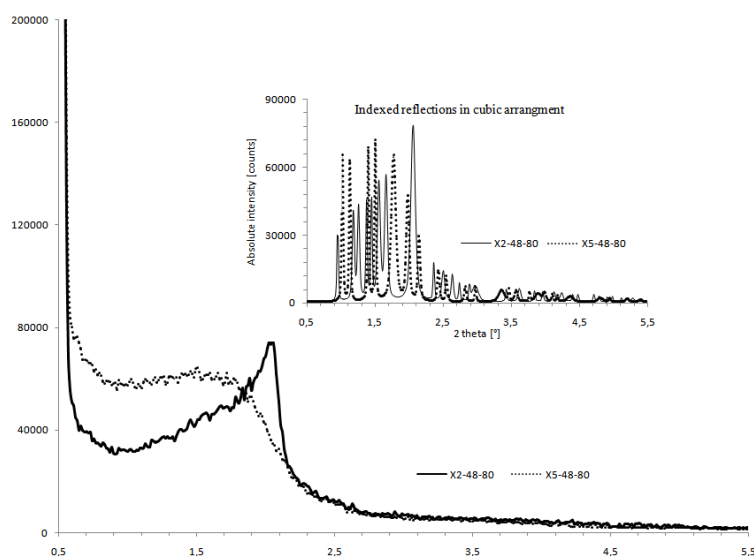
Table 1. Physicochemical properties of surfactants di-block copolymer type commercialized under the designation Brij® S 100 and Triton™ X-114.

Commercial name	Chemical formula	Molar weight (g/mol)	HLB*
Brij® S 100 Polyoxyethylene (100) stearyl ether	$C_{18}H_{37}(OCH_2CH_2)_{100}.OH$	4670	18
Triton™ X-114 Polyethylene glycol <i>tert</i> -octylphenyl ether	$C_{14}H_{21}(OCH_2CH_2)_8.OH$	647	13.5

* hydrophilic-lyophilic balance

Table 2. Textural and structural parameters of materials calcined at 550°C under air for 6 hours.

Designation	Surfactant mass ^f	$D_{\text{pore-pore}}^a$ (nm)	S_{BET} (m ² /g)	V_p^b (cm ³ /g)	ϕ^c (nm)	Wall Thickness ^d (nm)
BG-6-1	6g Brij® S 100; 24h; 100°C	6.97	999 (163) ^e	0.94 (0.07)	4.78	2.19
BG-3-1	3g Brij® S 100; 24h; 100°C	6.22	896 (498) ^e	1.27 (0.23)	3.77	2.45
X2-48-80	2g Triton™ X-114; 48h; 80°C	4.28	910 (801) ^e	0.69 (0.59)	3.04	1.24
X5-48-80	5g Triton™ X-114; 48h; 80°C	4.24	809 (759) ^e	0.39 (0.34)	1.92	2.32

^a Corresponding to the d value of the characteristic X-ray reflection of the calcined products.^b Calculated at P/P=0.99.^c Pore diameter calculated from 4V/S by BET method.^d Wall thickness= $D_{\text{pore-pore}} - \phi$.^e Microporous surface or volume.^f Used with 30g of H₂O: 120 ml HCl:9 g TEOS.**Figure 1.** Low-angle XRD patterns of calcined samples from Triton X114-TEOS system.

method using the Halsey equation for multilayer adsorption for all samples. Morphology and particle size of the final products were observed

by using scanning electron microscopy FE-SEM (JEOL JSM-6340F) operating at an acceleration voltage of 20–30 kV. Transmission electron

microscopy (TEM) images of the mesostructures were obtained from ultrathin sections (~50 nm) of epoxy resin-embedded samples.

4. Extraction of creatinine

To determine the concentration of creatinine (2-Amino-1-methyl-5H-imidazol-4-one; $C_4H_7N_3O$; N° CAS 60-27-5), blood samples were collected by venipuncture at the crease of the elbow in fasted subjects. The blood is subsequently collected into heparin tubes and labeled for each patient. The blood samples are centrifuged at a speed of 2,500 rpm for 10 min. Creatinine is titrated in biological fluids by the widely used colorimetric method [30, 31]. Samples of seven different male patients are made for the purposes of this study and the subjects are chosen from donors who undergo hemodialysis regularly. The plasma, obtained under high centrifugation of the blood sample, is poured onto the freshly prepared and calcined solid sample. The analysis is carried out by apparatus Unicel DxH 800, Beckman Coulter, after contact times set at 1, 2, and 24 h by measuring the concentrations of creatinine respectively before and after contact of the solid to estimate the rate of creatinine extraction. The amount of solid used is fixed at 100 mg for each analysis by contact of 1,000 μ l of plasma.

Results and Discussion

The addition of proper concentrations of TEOS and nonionic surfactants pore-directing agents was found to be essential to obtain silica materials of ordered mesostructures in acid-free conditions. For all samples, XRD patterns recorded on calcined samples show the presence of a broad peak in the 2θ range of $1-4^\circ$. Thus, figure 1a shows the small-angle XRD patterns of calcined mesoporous silica materials prepared from TEOS/Triton X114, which exhibits single broad peak in the 2θ range of $0.5-3^\circ$, indicating a poorly ordered mesostructure lacking long-range structural order such as observed for mesostructured solids with worm-like pores [30]. This peak's treatment shows, in fact, the

presence of multiple reflections easily indexed in $m3m$ cubic lattice and, if the correlation distance deduced from the main XRD peak can be attributed to the pore-pore distance, the calculation gives a value of 42.8 \AA for both used amounts ($x = 2 \text{ g}; 5 \text{ g}$) of Triton X114 and significantly lower for synthesis with Brij® S100 (Table 2). Cubic arrangement of pores and worm-like mesoporous texture were clearly observed by TEM for both samples obtained from Triton X 114 and Brij® S100 (figure 2) that is usually observed with such surfactants [32, 33].

Nitrogen adsorption/desorption isotherms are type IV for samples obtained from Brij S100 but the shape is different as shown in figure 3; Higher quantities of adsorbed N_2 were observed for BG-6-1 with a hysteresis of type H2 suggesting narrow diameters at the extremities of pores while BG-3-1 sample displayed a significant uptake of N_2 at high relative pressures ($P/P_0 > 0.90$), a signature of a high degree of textural porosity. The corresponding isotherm of X2-48-80 material featured sharp inflection in the intermediate P/P_0 region, indicating the presence of uniform mesopore channels; otherwise, the corresponding isotherm of X5-48-80 sample was type I characteristic of the microporous solids since we noted a large horizontal bearing in almost the whole domain of P/P_0 . The very high surface areas ($> 800 \text{ m}^2/\text{g}$) and pore volumes (generally in the range $0.40-1.20 \text{ cm}^3/\text{g}$) measured from these isotherms (Table 2) were also characteristic of mesostructured materials. However, very high microporosity was observed in materials prepared from TEOS/Triton X114 couple which suggests probably an interconnection between micropores and mesopores.

The determination of creatinine concentration in samples of blood plasma, placed in contact with the freshly prepared materials and calcined beforehand, is given in Table 3 which includes all test results. Compared to a healthy subject ($C_0 = 0.07 \text{ mmole/l}$), the chosen concentrations are very high creatinine, and are significantly reduced after one hour of contact. Thus, for

Table 3. Extraction results of creatinine by adsorption from micro- and mesoporous materials calcined at 550°C under air for 6 hours; C_o initial creatine concentration; C_r remaining creatinine concentration; m_{ads} amount of creatinine adsorbed per gram of solid.

Contact time		1h	2h	24h	1h	2h	24h
Solids		BG-6-1			BG-3-1		
Control sample ($C_o=0.07\text{mmol/L}$)	C_r (mmol/L)	0.035	0.027	0.027	0.037	0.039	0.038
	n_{ads} ($\mu\text{mol/g}$)	0.34	0.41	0.41	0.33	0.30	0.31
Sample1 $C_o=0.71\text{mmol/L}$	C_r (mmol/L)	0.59	0.62	0.61	0.71	0.71	0.70
	n_{ads} ($\mu\text{mol/g}$)	1.16	0.94	1.01	-----	-----	0.53
Sample2 $C_o=0.62\text{mmol/L}$	C_r (mmol/L)	0.36	0.37	0.37	0.50	0.49	0.49
	n_{ads} ($\mu\text{mol/g}$)	2.50	2.57	2.57	1.22	1.33	1.33
Sample3 $C_o=0.68\text{mmol/L}$	C_r (mmol/L)	0.45	0.49	0.45	0.61	0.46	0.44
	n_{ads} ($\mu\text{mol/g}$)	2.24	1.89	2.22	0.63	2.20	2.23
Sample4 $C_o=0.52\text{mmol/L}$	C_r (mmol/L)	0.34	0.19	0.18	0.45	0.40	0.36
	n_{ads} ($\mu\text{mol/g}$)	1.73	3.24	3.37	0.65	1.12	1.56
Sample5 $C_o=0.45\text{mmol/L}$	C_r (mmol/L)	0.27	0.23	0.21	0.35	0.34	0.34
	n_{ads} ($\mu\text{mol/g}$)	1.82	1.92	1.80	0.99	1.05	1.09
solids		X2-8-80			X5-48-80		
Sample6 $C_o=0.49\text{mmol/L}$	C_r (mmol/L)	0.39	0.40	0.40	0.38	0.35	0.34
	m_{ads} ($\mu\text{mol/g}$)	0.99	0.94	0.94	1.1	1.45	1.55
Sample7 $C_o=1.02\text{mmol/L}$	C_r (mmol/L)	0.71	0.72	0.75	0.67	0.70	0.70
	m_{ads} ($\mu\text{mol/g}$)	3.11	2.99	2.63	3.46	3.18	3.20

sample 4 in contact with the BG-6-1 material, the extraction rate is estimated at 33.5% and 65.2% at 1 and 24 h respectively, which is equivalent to 1.73 and 3.37 μmole of creatinine extracted per gram of solid. Figure 4 indicates that the maximum rate of extraction is reached after 2 hours for BG-6-1 material. There is no correlation between the initial creatinine concentration and the mass extracted from creatinine. However, we note that beyond a concentration of 0.52 mmol/l, a significant decline in the rate of extraction of creatinine. Adsorption capacities depend on both, the texture of the material and the initial content of creatinine; for the same plasma sample and in the same operating conditions, it is found that materials which exhibit a significant microporosity as the X2-48-80 and X5-48-80 solids are those which adsorb more creatinine; it

is likely that the organic molecule is trapped easily in the micropores after crossing the mesopores when they can. Moreover, with the same materials, the extraction rate is higher if the creatinine content is large initially in the plasma. This is not verified for other strictly mesoporous materials BG-6-1 and BG-3-1 where it is assumed that the creatinine molecule can both adsorb and desorb without geometric constraints of the pores.

Furthermore, it is stated that, during these analyzes, the urea is not extracted by these purely silica materials and whose surface consists essentially of siloxane and silanol bonds. Indeed, Silica being relatively simple and unreactive, can be thought of as a "pegboard" [34]. The functional groups that terminate silica include -OH groups, believed to occur in the

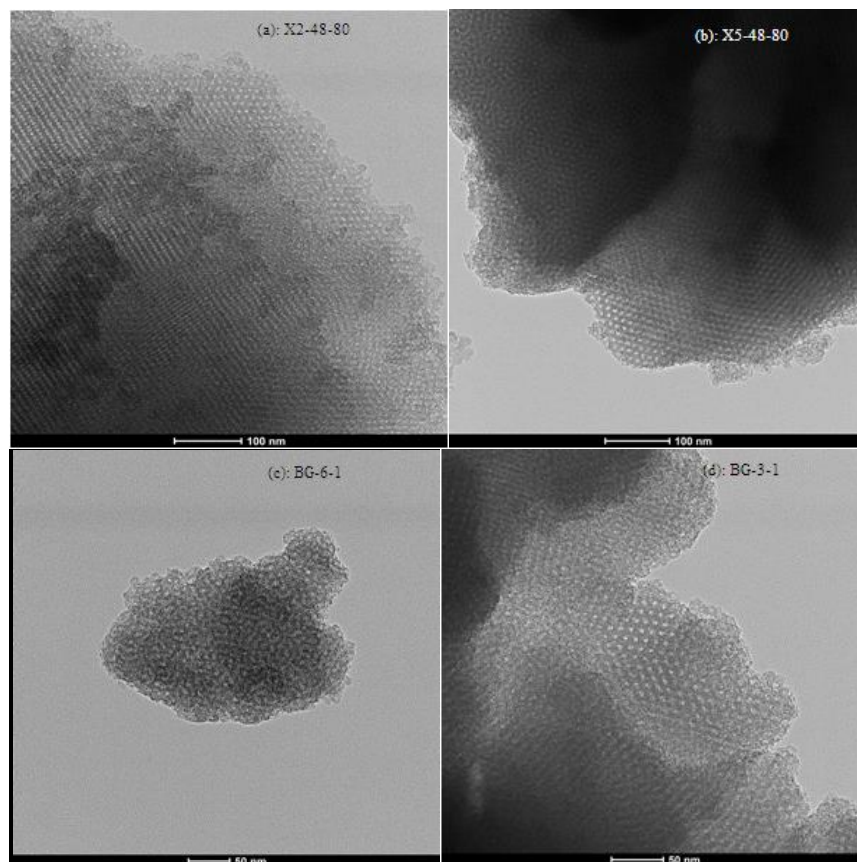


Figure 2. TEM image of wormhole pore structure and cubic arrangement of the calcined samples prepared from TEOS and: (a, b) Triton X-114; (c, d) Brij S100.

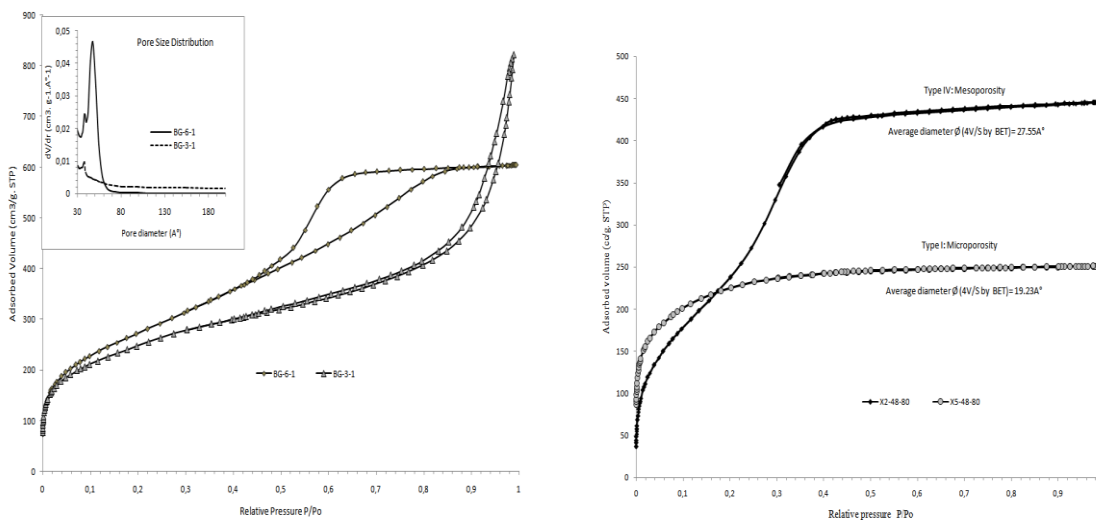


Figure 3. Nitrogen adsorption-desorption isotherms for the calcined samples formed from TEOS and: (a) Brij S100; (b) Triton X114 under acidic conditions. The insert provides the 4V/S pore size distributions.

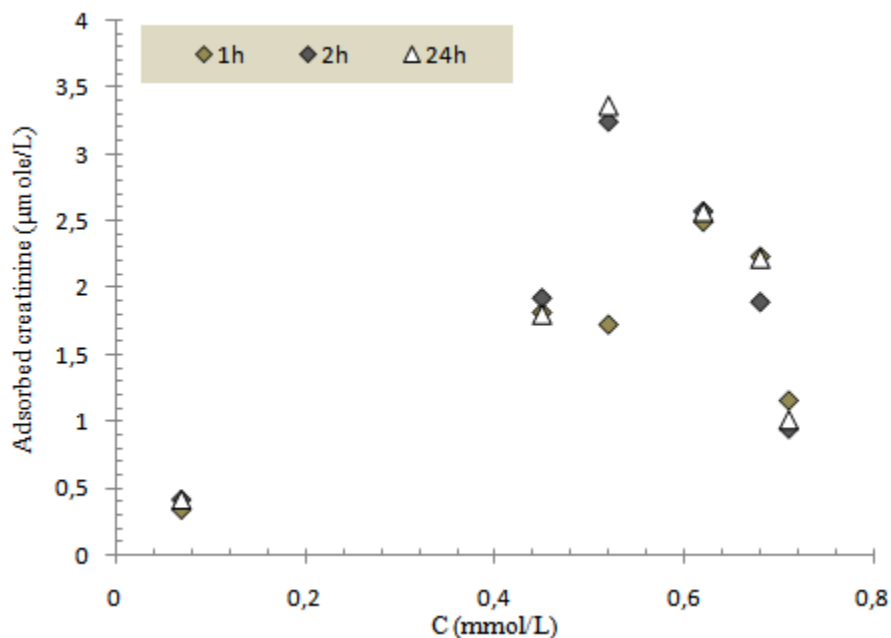


Figure 4. Isotherm of adsorption creatinine/ BG-6-1.

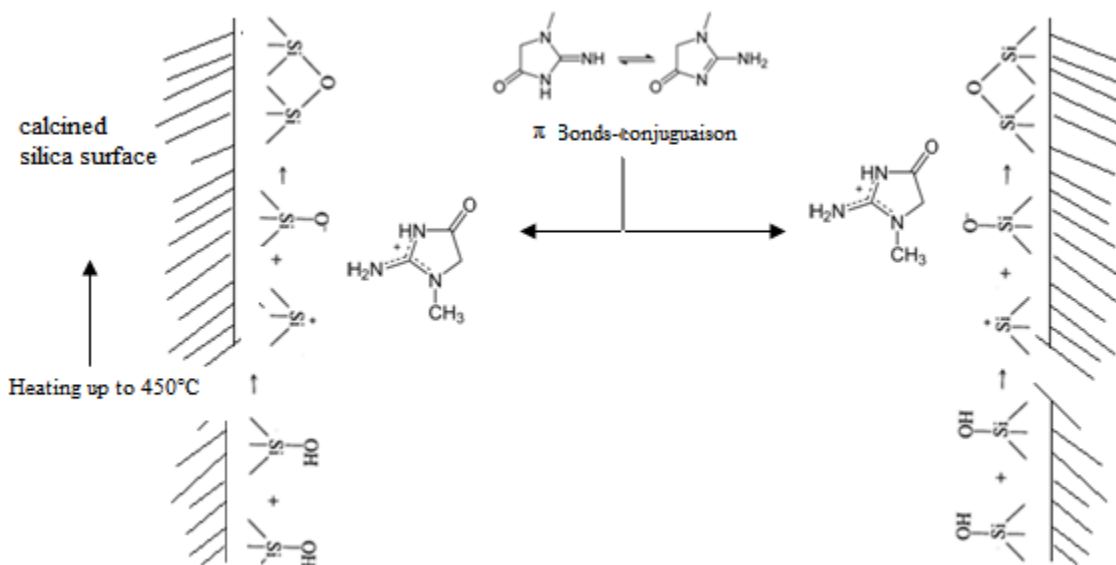


Figure 5. Mechanism of creatinine physisorption onto purely silica surface.

following scheme as shown in figure 5. When the surface is heated, water is driven off; and if the temperature is raised to about 450+°C, stable and relatively unreactive “siloxane bonds” are formed. Taking advantage of the reactivity of

these groups, which are weakly acidic ($pK_a = 7$) one can attach many kinds of organic molecules.

Since urea is a very thermodynamically stable molecule and the interactions are weak at the

silica surface, it is easy to understand the absence of adsorption of urea, but not for creatinine molecule which has a delocalized π bond between the nitrogen atoms of the pentavalent cycle of her configuration. The interactions between the charged poles which occur at the surface, however weak, are responsible for the creatinine physisorption. This probable mechanism is based on a partial deprotonation of the molecule which keeps it fixed onto the surface.

To conclude, we have shown that creatinine is extracted in the presence of various forms of purely silica materials. Preliminary tests showed that the pore size, specific area surface and volume pore have a major influence on physisorption molecule. In the case of our experiments, we can conclude that the presence of micropores greatly favors the adsorption and probably silica-oxygen surface groups that are located on the surface are responsible for the interactions that allow creatinine fixation. Nowadays, there is a fast progress in application of amorphous micro- and mesoporous silica in medicine and biology. Therefore, one should be used into account the possibility of elimination different toxins in the presence of these materials.

Acknowledgments

This work is part of research project CNEPRU (Oran-1 University) of the Ministry of Higher Education which has provided us with financial support; the financial support of the General Directorate of Scientific Research and Technological Development (DGRSDT). The University of Almeria is gratefully acknowledged for characterization analyzes reported in this work.

Reference

1. Bergé-Lefranc D, Schaft O, Denoyel R et al. 2010. Adsorption properties of zeolites for artificial kidney applications. *Microporous and Mesoporous Materials*. 119: 144-148.

2. Lu Y, Fan H, Stump A, Ward TL, Rieker T, Brinker CJ. 1999. Aerosol-assisted self-assembly of mesostructured spherical nanoparticles. *Nature*. 398: 223-226.
3. Wernert V, Schaft O, Ghobarkar H, Denoyel R. 2005. Adsorption properties of zeolites for artificial kidney applications. *Microporous and Mesoporous Materials*. 83: 101-113.
4. Koubaissy B, Toufaily J, Yaseen Z. 2017. Adsorption of uremic toxins over dealuminated zeolites, *Adsorption Science and Technology*. 35: 3-19.
5. Cao Y, Gu Y, Wang K. 2016. Adsorption of creatinine on active carbons with nitric acid hydrothermal modification. *Journal of the Taiwan Institute of Chemical Engineers*. 66: 347-356.
6. Huang R, Liu Z, Sun B. 2016. Preparation of dialdehyde cellulose nanocrystal as an adsorbent for creatinine. *Canadian Journal of Chemical Engineering*. DOI: 10.1002/cjce.22306.
7. Kresge CT, Leonowicz ME, Roth WJ, Vartuli JC, Beck JS. 1992. Ordered mesoporous molecular sieves synthesized by a liquid-crystal template mechanism. *Nature*. 359: 710-712.
8. Namekawa K, Tokoro Schreiber M, Aoyagi T, Ebara M. 2014. Fabrication of zeolite-polymer composite nanofibers for removal of uremic toxins from kidney failure patients. *Biomater. Sci*. doi: 10.1039/c3bm60263j.
9. Takai R, Kurimoto R, Nakagawa Y, Kotsuchibashi Y, Namekawa K, Ebara M. 2016. Towards a Rational Design of Zeolite-Polymer Composite Nanofibers for Efficient Adsorption of Creatinine. *J of Nanomaterials*. <http://dx.doi.org/10.1155/2016/5638905>.
10. Lou P-J, Chiu Y, Chou CC, Liao B-W, Young T-H. 2010. The effect of poly(ethylene-co-vinyl alcohol) on senescence associated alterations of human dermal fibroblasts. *Biomaterials*. 31: 1568-1577.
11. Young T-H, Lin C-W, Cheng L-P, Hsieh C-C. 2016. Preparation of EVAL membranes with smooth and particulate morphologies for neuronal culture. *Biomaterials*. 22: 1771-1777.
12. Kotsuchibashi Y, Ebara M. 2016. Facile functionalization of electrospun poly(ethylene-co-vinyl alcohol) nanofibers via the benzoxaborole-diol interaction. *Polymers*. 8: 11. doi:10.3390/polym8110380.
13. Kresge CT, Leonowicz ME, Roth WJ, Vartuli JC, Beck J. S. 1992. Ordered mesoporous molecular sieves synthesized by a liquid-crystal template mechanism. *Nature*. 359: 710-712.
14. Beck JS, Vartuli JC, Roth WJ, Leonowicz ME, Kresge CT, Schmitt KD, Chu CTW, Olson DH, Sheppard EW, McCullen SB, Higgins JB, Schlenker JL. 1992. A new family of mesoporous molecular sieves prepared with liquid crystal templates. *J Am Chem Soc*. 114: 10834.
15. Yanagisawa T, Shimizu T, Kuroda K, Kato C. 1990. The preparation of alkyltrimethylammonium-kanemite complexes and their conversion to microporous materials. *Bull Chem Soc Jpn*. 63: 988-992.
16. Inagaki S, Fukusima Y, Kuroda K. 1993. Synthesis of highly ordered mesoporous materials from a layered polysilicate. *J Chem Soc Chem Commun*. 680: X029. DOI: 10.1039/C399300FX029.
17. Corma A. 1997. From microporous to mesoporous molecular sieve materials and their use in catalysis. *Chem Rev*. 97: 2373-2420.
18. Ying JY, Mehnert CP, Wong MS. 1999. Synthesis and applications of supramolecular-templated mesoporous silica. *Angew. Chem. Int Ed*. 38: 56-77.
19. Barton TJ, Bull LM, Klemperer WG, Loy DA, Mcenaney B, Misono M, Monson PA, Pez G, Scherer GW, Vartuli JC, Yaghi OM. 1999. Tailored porous materials. *Chem Mater*. 11: 2633-2656.
20. Tanev PT, Pinnavaia TJ. 1995. A neutral templating route to mesoporous molecular sieves. *Science*. 267: 865-867.

21. Tanev PT, Pinnavaia TJ. 1996. Mesoporous Silica Molecular Sieves Prepared by Ionic and Neutral Surfactant Templating: A Comparison of Physical Properties. *Chem Mater.* 8: 2068-2079.
22. Bagshaw SA, Prouzet E, Pinnavaia TJ. 1995. *Science.* 269: 1242-1243.
23. Bagshaw SA, Kemmitt T, Milestone N. 1998. Microporous Mesoporous *Mater.* 22: 419-422.
24. Prouzet E, Pinnavaia TJ. 1997. Assembly of Mesoporous Molecular Sieves Containing Wormhole Motifs by a Nonionic Surfactant. *Angew Chem Int Ed Engl.* 36: 516-518.
25. Boissière C, Larbot A, Van der Lee A, Kooyman PJ, Prouzet E. 2000. A New Synthesis of mesoporous MSU-X Silica Controlled by a Two-Step Pathway. *Chem Mater.* 12: 2902-2905.
26. Boissière C, Larbot A, Prouzet E. 2000. Synthesis of Mesoporous MSU-X Materials Using Inexpensive Silica Sources. *Chem Mater.* 12: 1937-1940.
27. Prouzet E, Cot F, Nabias G, Larbot A, Kooyman P, Pinnavaia TJ. 1999. Assembly of Mesoporous Silica Molecular Sieves Based on Nonionic Ethoxylated Sorbitan Esters as Structure Directors. *Chem Mater.* 11: 1498-1503.
28. Kim JM, Sakamoto Y, Hwang YK., Kwon YU, Terasaki O, Park S-E, Stucky GD. 2002. Structural Design of Mesoporous Silica by Micelle-Packing Control Using Blends of Amphiphilic Block Copolymers. *J Phys Chem B.* 106: 2552-2558.
29. Larsen K. 1972. Creatinine assay by a reaction-kinetic principle. *Clin Chim Acta.* 41: 209-217.
30. Henry JB. 1984. *Clinical Diagnosis and Management by Laboratory Methods.* 17th ed. Philadelphia: WB Saunders.
31. Pauly TR, Pinnavaia TJ, 2001. Pore Size Modification of Mesoporous HMS Molecular Sieve Silicas with Wormhole Framework Structures, *Chemistry of Materials.* 13,3: 987-993
32. Kim S-Su, Pauly TR, Pinnavaia TJ. 2000. Non-ionic surfactant assembly of wormhole silicamolecular sieves from water soluble silicates. *Chem Commun.* 2000: 835-836.
33. Chalal N, Bouhali H, Hamaizi H, LeBeau B, Bengueddach A. 2015. CO₂ sorption onto silica mesoporous materials made from nonionic surfactants. *Microporous and Mesoporous Materials.* 210: 32-38.
34. Boehm HP, Knozinger H. 1983. *Catalysis-Science and Technology*, J. R. Anderson and M. Boudart, eds. Springer Verlag, Berlin, 1983.